F-39-17

SAE The Engineering Society For Advancing Mobility Land Sea Air and Space

400 COMMONWEALTH DRIVE, WARRENDALE, PA 15096

AEROSPACE RECOMMENDED PRACTICE

ARP4252

Issued 7-1-89

Submitted for recognition as an American National Standard

INSTRUMENTAL METHODS OF DETERMINING SURFACE CLEANLINESS

1. SCOPE:

1.1 Scope: This Aerospace Recommended Practice is intended as a guide toward standard practices for the determination of surface cleanliness that are applicable to field operation. Some of these methods can also be used to determine quality assurance that a surface has been properly prepared and maintained.

The instrumental methods are: Wettability, Surface Potential Difference (SPD), Ellipsometry, and Optically Stimulated Electron Emission (OSEE). Each instrument is described with respect to measurement techniques, limitations, and advantages and types of available instruments. Elementary theoretical principles and examples of the use of each instrument are also given.

1.2 Application: The application of the instruments recommended here is to establish that the state, or quality, of a surface is satisfactory for its intended use. Surface cleanliness refers to the absence of materials that would degrade the surface with respect to its intended use. In the case of adhesive bonding, the contamination is usually organic oils or greases; for soldering, welding, coating, or plating, it may be oxide or hydroxide films; for painting it may be water condensate. For example, for adhesive bonding, a properly prepared metal surface may require a hydroxide film that is stable with respect to heat and moisture. The presence of an oxide or hydroxide film that is not stable to heat and moisture, or that is mechanically weak, would be considered a contaminant.

2. INSTRUMENTS: The type of instrument recommended for surface qualification will depend upon factors such as: the amount of information needed, the frequency of need of information, and whether samples of specified size and shape need be inserted into the instrument or if the sensor can be placed on or near the actual surface of interest. Other considerations are: cost of the instrument, maintenance requirements, and needed operator training. Table 1 gives a comparison of the various types of instruments as to: principles of operation, what is measured, approximate depth of measurement, field of application, estimated proficiency level to operate, estimated proficiency level to interpret results, and estimated cost range.

2.1 Wettability Tests:

2.1.1 Measurement Techniques:

2.1.1.1 There are two wettability tests in use. They are the "Water Break Test" and the "Hydrophobic Surface Films by the Atomizer Test." The most common method for the determination of the surface cleanliness has been the "Water Break Test" (ASTM F22). This test simply entails placing a drop of clean water on the surface and observing whether the water spreads. It is assumed that if the water spreads, the surface is clean and is proper for the intended use (e.g., adhesive bonding, soldering, plating, etc.). However, the test only indicates that the attraction between water molecules and surface atoms is sufficient to overcome the attraction of water molecules to themselves (i.e., overcome the liquid surface tension).

2.1.1.2 The reason the "Water Break Test" has been so useful, is that the most common surface contamination has been nonpolar organic oils and greases, which have a very low attraction for highly polar water molecules. The polar nature of a molecule is simply related to the distance of separation between the positive charge of the atomic nucleus and the net negative charge of the orbiting electrons. A quantitative expression of this is given in the dipole moment of molecules which will be more fully described in the Surface Potential Difference method.

2.1.1.3 Since oils and greases are usually nonpolar, they have weak attraction to themselves and to other molecules; consequently, they can slip past each other and separate easily, making good lubricants, but poor adhesives.

2.1.1.4 The "Hydrophobic Surface Films by the Atomizer Test" (ASTM F21), deemed a hundred times more sensitive than the "Water Break Test," involves the spray of a water mist on the surface and the observation of whether or not water droplets form.

2.1.2 Limitations and Advantages:

2.1.2.1 The wettability tests are limited to the detection of nonpolar contamination that results in an observable contact angle. There are many materials that are polar enough to reduce the contact angle (Θ) to zero but still degrade the surface with respect to its intended use. For example, strong, environmentally durable adhesive joints may require strong, stable, hydroxide layers. This is the case for adhesive bonding of aluminum and titanium parts for aerospace purposes. Weak unstable oxide or hydroxide layers may be very wettable but totally unsuitable for bonding.

2.1.2.2 Another limitation is the difficulty of automated measurement in the field. The techniques are primarily performed by a person and are subject to human error.

2.1.2.3 These techniques give no information about the elemental content of the contamination, other than its polar nature.

2.1.2.4 The wettability tests are limited to high energy surfaces such as metals, ceramics, or glasses. They are not suitable for low energy surfaces, such as most plastics and some composites.

2.1.2.5 The wettability tests may be a source of contamination, in that the presence of water, or contaminants within the water, could be detrimental.

2.1.2.6 It should be pointed out that when it may be required to test the underside of aircraft for cleanliness, the "Water Break Test" is difficult.

2.1.3 Available Instruments:

2.1.3.1 The simplest method for surface cleanliness testing is the use of an atomizer, a syringe, pipette, or any container for dispensing clean water onto a surface, followed by visual observation of whether the water beads up or spreads.

2.1.3.2 Reflective goniometers to measure liquid contact angles are available to observe the shape of the side view of the drop as in Figure 1a, for a drop with Θ 90 degrees and Figure 1b for a drop with Θ 90 degrees. A protractor eyepiece is provided so that a hair line can be aligned with the tangent to the curvature of the drop, at the liquid-solid intercept. The contact angle is read directly from the protractor scale. The goniometer usually has an environmental chamber so the contact angle can be measured with controlled temperature and environment.

2.2 Surface Potential Difference (SPD):

2.2.1 Measurement Techniques:

2.2.1.1 If two parallel metal plates are connected by a conductor, an electric field is formed between them due to the difference in the work function between them. The work function is the energy needed to remove electrons from within the metal. If one of the plates is used as a reference electrode, i.e., constant with time and other measurement conditions, then changes in the potential between the reference electrode and the measurement surface reflect the changes in the work function of the measurement surface. The difference in potential between the two electrodes is referred to as the contact potential difference (CPD), and any changes that take place in the work function of the measurement surface is referred to as its surface potential difference or SPD.

2.2.1.2 There are two SPD measurement techniques: (1) the vibrating capacitor (known as a Kelvin probe), and (2) a technique for which the reference electrode has a layer of radioactive material, such as polonium or americium 241. The radioactive material is covered with a thin layer of metal to prevent leakage of the radioactivity.

2.2.1.3 The reference electrode is placed near the surface that is to be measured for cleanliness, and a voltmeter connected between the measurement surface and the reference electrode is observed and recorded. If the voltmeter is connected to a recorder or the data acquisition components of a computer, a permanent record of SPD can be attained as a function of the sample, of the position on a sample, or with respect to time.

2.2.1.4 The distance that the reference electrode must be held with respect to the surface is determined by observing the voltage as the probe nears the surface. As the probe approaches within a critical distance, the voltage remains constant. The critical distance depends on a number of factors, such as radioactivity level in the radioactive method, or the vibration frequency in the Kelvin method, but is usually of the order of a few millimetres, so that, although the measurements are made without contact, great care with respect to positioning is usually not necessary.

2.2.1.5 As for all methods for determining surface cleanliness, SPD can be used for surface quality assurance by empirical means, without much understanding for instrument principles or theory. Measurements are made for a set of samples, that are known to be satisfactory, to obtain an acceptance window or range. This window is expanded so that acceptable surfaces are not rejected. Then surfaces that do not fall within the acceptance window are rejected or routed for further preparation.

2.2.2 Limitations and Advantages:

2.2.2.1 In general, contamination by nonpolar greases or oils will increase SPD, but as for wettability measurements, this cannot be used as a sure measure of surface quality.

2.2.2.2 SPD gives no information as to elemental composition of contamination.

2.2.2.3 In order to measure SPD, it is assumed that during the time of measurements the reference electrode does not change, so that SPD = change in CPD. This is usually not the case and one can never be sure which electrode is changing. In reference 1, reference electrodes made of nickel, polytetrafluoroethylene (PTFE) sprayed nickel, as well as gold and platinum showed some drift with time.

2.2.2.4 Although the radioactive SPD instrument is simple to operate, it has the disadvantage that a state license is required for the use of radioactive material. The vibrating electrode, although considerably more complicated, can be used without a license.

2.2.2.5 SPD has the advantage over wettability in that it can be automated, relying less on human judgement. The sensor is small and can be taken to the surface of interest. Although SPD is theoretically limited to the surface monolayer, indirect relationships exist between SPD and much thicker films. For example, a linear relationship exists between SPD and hydroxide film thicknesses to 720 nm (7200 Å) on aluminum (See Figure 8). There must be a direct correlation between the surface dipole structure and anodize voltage, just as there is a direct correlation between the anodic film thickness and voltage.

2.2.2.6 The SPD probe does not touch the surface it is measuring and is therefore a nondestructive, noncontaminating source.

2.2.2.7 Given sufficient calibration with respect to surfaces and anticipated contamination, SPD can be a useful surface inspection technique.

2.2.3 Available Instruments:

2.2.3.1 Figure 2a is a schematic equivalent circuit diagram for the radioactive SPD technique. The current "i" flowing in the circuit can be expressed by Ohm's law:

$$i=CPD/(R+r)=e/r \qquad (1)$$

where CPD is the contact potential difference, R is the air gap resistance between the sample surface and the reference electrode, r is the electrometer resistance, and e is the electrometer voltage reading. A radioactive substance, sealed behind a metal foil on the reference electrode, is used to provide ionization of the air between the electrodes, thus reducing R such that R r. In this case:

$$i=CPD/r=e/r \qquad (2)$$

and CDP=e, the electrometer reading. To demonstrate that R r, e is measured as a function of distance between the electrodes. As long as e is independent of distance, R r.

2.2.3.2 Figure 2b shows a schematic equivalent circuit for the vibrating electrode SPD instrument. The vibrating capacitor is connected in series with a resistor R and a voltage source $E_O + E_R$. In general, for $E_O + E_R = O(V)$, an electric field will exist in the gap between the plates of the capacitor because CPD is not zero. The sinusoidal variation of the capacitor spacing will lead to an alternating current in the external circuit. To determine CPD, $E_O + E_R$ is varied until there is no currrent flowing in the external circuit and hence no field in the gap. At this null point, $E_O + E_R$ is equal to CPD. The voltage V developed across R is:

$$V_O = \frac{\varepsilon_O A \alpha \omega R}{d_O} f(CPD - E_O - E_R) \cos\omega t \text{ for } V_O \quad (CPD - E_O - E_R) \qquad (3)$$

where d_O is the mean capacitor spacing, $d_O\alpha$ is the amplitude of vibration at the frequency ω and A is the area of the plates. Since Vo is proportional in magnitude and sign to $(CPD - E_O - E_R)$, it can be used as an error signal for a simple servomechanism. The phase sensitive detected DC signal proportional to $(CPD - E_O - E_R)$ is applied as the bucking voltage $E_O + E_R$. The feedback is negative and continous balance is maintained with the output voltage given by

$$E = (CPD - E_R)/(1 + 1/G) \qquad (4)$$

where G is the open loop gain. This servomechanism was first used by Palevsky[2] in a vibrating capacitor electrometer.

2.3 Ellipsometry:

2.3.1 Measurement Techniques:

2.3.1.1 An ellipsometer is an optical instrument that measures the ellipticity of a beam of monochromatic light that reflects from the surface of interest. The incident beam passes through a polarizer, through a compensator (quarterwave plate), reflects from the surface, and finally passes through another polarizer (referred to as the analyzer) into a photodetector.

2.3.1.2 Plane polarized light can be resolved into two beams that are at right angles (orthogonal). The orthogonal beams are in phase and thus the resultant plane polarized beam remains in the same plane as it propagates through space. If no compensator is present, the surface will cause the reflected orthogonal beams to be out of phase. Thus the reflected beam vector rotates as it propagates. The projection of the rotating reflected beam is an ellipse with major and minor axes that represent the amplitude of the orthogonal components. The orientation of the ellipse represents the phase shift of the orthogonal components.

2.3.1.3 An ellipsometer measures the ellipticity of the reflected beam, as two parameters, tan ψ, which is the ratio of the amplitudes of the orthogonal components, and Δ, which is the phase shift of these components that results from reflection.

2.3.1.4 The elliptically polarized light carries with it information about the surface from which it was reflected. If the surface is absolutely clean, the refractive index of the surface can be computed from Δ and ψ. If a thin film is present, the thickness and refractive index of the film can be computed. Ellipsometers are remarkable with respect to the sensitivity the phase shift has with film thickness. In fact, the phase shift Δ is so sensitive that one thousandth of one monolayer of oxide on metals can be detected. However, ellipsometers are usually used to measure film thickness in the range 0 to 6000 nanometres.

2.3.1.5 The refractive index of a surface or a film is a complex number represented as

$$\hat{N} = N(1-i\chi) \qquad (5)$$

where N, the real part of the complex number is the refractive index, which measures the refraction or change of direction of the light as it passes from the ambient into the material and χ, the imaginary part is the absorption index, which measures the fraction of the light that is absorbed as it passes in and out of the material upon reflection.

2.3.1.6 Figure 3 shows a plot of Δ vs ψ for a theoretical film (solid curve) on aluminum. The ticks and corresponding numbers on the curve indicate the thickness (in Å) of a transparent film of index N = 1.3, χ = 0. The solid points in Figure 3 are the measured values of Δ and ψ for an aluminum mirror.

The point 0 (V) shows the original oxide to be about 15 nm (150 Å). At 2(V) anodize, the thickness is about 80 nm (800 Å); at 4(V), about 175 nm (1750 Å); and at 6(V) about 325 nm (3250 Å).

2.3.2 Limitations and Advantages:

2.3.2.1 At 8(V) the film thickness in Figure 3 is not 45 nm, but about 350 + 45 or 395 nm. The value of thickness at which the Δ, ψ values begin to repeat is called the first order film thickness and points out a limitation for an ordinary ellipsometer. To determine the film thickness one must know the order of the film. This limitation is removed by measuring at two wave lengths or two angles of incidence.

2.3.2.2 The theory of ellipsometry is limited to films of uniform refractive index on perfectly smooth substrates. Perhaps the most difficult limitation of the interpretation of ellipsometry is the effect of roughness. However, roughness does not prevent precision measurements from being made. An example is given in Figure 4 for aluminum samples that had been etched (very rough) in sulfuric-acid-dichromate solution and then anodized in phosphoric acid solution at various voltages.

2.3.2.3 It is observed that the Δ, ψ data go around a loop as in Figure 3, but the loop is distorted due to the roughness. A comprehensive analysis on the effect of roughness on ellipsometry can be found in Ref. 3.

2.3.3 Available Instruments:

2.3.3.1 There are four types of commercially available instruments. These are the nulling type, the rotating analyzer type, the comparison type, and the TRI-BEAM type. The nulling type is represented in Figure 5a. The manually operated nulling ellipsometer is the most precise instrument available. Typically these instruments have verniers that allow reading of Δ and ψ to 0.01 degree. There are automated nulling ellipsometers which typically measure Δ to 0.1 degree and ψ to 0.05 degree.

2.3.3.2 The second type, the rotating analyzer ellipsometers, takes light intensity data as the analyzer rotates through 360 degrees. From light intensity data vs analyzer azimuth, values of Δ and ψ are calculated and typically resolve to 1.0 and 0.5 degree, respectively.

2.3.3.3 The third type, the comparison ellipsometer, has the arrangement in Figure 5b. This ellipsometer utilizes polarized white light and makes a direct visual comparison between a test surface and a reference standard that has known properties. There are no moving parts. The operator looks through the analyzer and sees rainbow hues where the two surfaces are dissimilar and a total extinction of light where the two surfaces have identical properties. The dark extinction line is compared to a scale that indicates the film thickness.

2.3.3.4 An advantage of the comparison ellipsometer is that the film thickness is read directly, with no computer calculations needed. A severe disadvantage is that a wedge-shaped film standard is necessary, with identical index of refraction to that of the sample to be measured. This type of ellipsometer does not measure refractive index as do the other types.

2.3.3.5 The fourth type, the TBE (tri-beam) ellipsometer, is based on the analysis of Ref. 4. The principle is similar to the rotating analyzer, except that the intensity of light is monitored at 0 degree, 45 degree and 90 degree azimuth of the analyzer. There are no moving parts in the ellipsometer and all light intensity readings are automatically entered into a computer via an A/D converter. The computer calculates Δ and ψ from the three intensities and then calculates film thickness and refractive index. All the other ellipsometer types must have samples produced and placed in the ellipsometer. This prevents measurements being made directly on production lines or on large production parts. The three-intensity type ellipsometer has a small hand held sensor that can be placed on production lines or scanned over large production parts.

2.3.3.6 Except for the comparison ellipsometer, the typical measurement time varies from 5 to 50 seconds per measurement. Due to having no moving parts and being entirely electronic and computer controlled, the TBE (tri-beam) type ellipsometer can make measurements at about 0.001 seconds per measurement, or as fast as the computer can take the data. This has the advantage that two dimensional surface mapping can take place in a relatively short time. For example, a map of 1000 data points can be made in a matter of seconds as compared to hours for the other ellipsometers.

2.4 Optically Stimulated Electron Emission (OSEE):

2.4.1 Measurement Techniques:

2.4.1.1 An OSEE instrument has a sensor that contains a lamp that emits ultraviolet (UV) light and a collector for collecting electrons emitted by the surface. The UV light stimulates the emission of electrons from the surface. The electrical current resulting from the electron emission is composed of electrons and molecules that capture electrons to become negative ions.

2.4.1.2 The use of OSEE for surface inspection relates the high sensitivity of electron emission to contaminants on the surface. As for SPD and Ellipsometry, OSEE is restricted to a very thin surface layer (~ 0 to a few hundred Angstroms) that will allow electrons to escape. As for SPD, thicker layers can affect the emission and attenuation characteristics of the outer layer in a systematic way, and thus make OSEE useful for the measurement of the thicker films.

2.4.1.3 The position of the OSEE with respect to the surface is not critical and can vary from millimetres to centimetres. However, once an appropriate distance has been chosen, it must be maintained for further measurements because the current is attenuated by the gas between the electrodes.

2.4.1.4 The OSEE instrument can be used as a quality assurance tool with very little knowledge of the theoretical principles or details regarding its function. As mentioned for SPD, samples of known utility can be used to obtain an acceptance window and after expanding the window to eliminate rejection of acceptable parts, signals outside of the acceptance window can be used to reject unacceptable parts.

2.4.1.5 The electronic signal from the OSEE instrument can be given directly to a computer via an A/D converter and peripheral interface adaptor (PIA), for data acquisition management, or to operate automated corrective action apparatus.

2.4.2 Limitations and Advantages:

2.4.2.1 OSEE has one important limitation, that of surface changes due to exposure to the UV light. This can be overcome, in most cases, by minimization of the exposure. It is well known that exposure of the surface to UV light can be used to clean a contaminated surface. The UV light produces ozone which reacts with hydrocarbon contamination to form carbon monoxide and carbon dioxide, which leave the surface as gas.

2.4.2.2 Another limitation relates to the surface depth of UV penetration and electron escape.

2.4.2.3 OSEE does not reveal information as to the elemental composition of surface layers, but might be useful in this regard with extensive calibration studies.

2.4.2.4 Due to the mechanism of electron and ion current flow through the air, and the effect of distance on the electric field between the surface and the collector, measurements must be made with a constant distance between the probe and the surface for reproducibility. This is usually easily achieved.

2.4.3 Available Instruments:

2.4.3.1 There is only one type of OSEE instrument presently available. As for the other instruments, the physical configuration (See Figure 6) is simple, but the actual development of a reliable, low noise instrument is complex and difficult.

3. THEORETICAL PRINCIPLES AND EXAMPLES:

3.1 Wettability Tests:

3.1.1 Theoretical Principles:

3.1.1.1 The contact between a liquid and solid is defined by Figure 1. Zisman and coworkers[5] have developed detailed procedures for experimental measurement of liquid-solid contact angles. Zisman showed that a plot of Cos r versus liquid surface tension q, for a homologous liquid series against a common solid, tends to produce a linear curve. Extrapolation of the Cos r versus q to Cos r = 1 defines a critical liquid surface tension, q_c, for wettability of the solid. Any liquid with surface tension less than the critical surface tension will spread on the solid surface (i.e., r = 0).

3.1.1.2 The energy to separate a liquid from a solid is referred to as the work of adhesion, Wa, and is related to r and q by the following equation:

$$Wa=q(1+\text{Cos } r) \qquad (6)$$

From Eq. (6) it is observed that since the contact angle can vary from 0 to 180 degrees, Wa must be at least 2q. The strength of adhesion, or the bond between molecules in the liquid and molecules or atoms in the solid, can be estimated by measuring the contact angle and obtaining the liquid surface tension from the handbooks for physics and chemistry. However, since r cannot be less than zero, the strength of the bonds that are greater than 2q cannot be determined this way.

3.1.1.3 The theory for the "Atomizer Test" is essentially the same as for the "Water Break Test," except that the water is placed on the surface as extremely small droplets or mist.

3.1.2 Wettability Examples:

3.1.2.1 Figure 7 indicates that a single layer, two molecules thick (from 1 dip), of a natural grease (myristic acid) can increase the contact angle from approximately zero to over 90 degrees for a smooth aluminum mirror. The contact angle does not change after the first dip because each dip deposits a bilayer with a polar acid group sandwiched between the nonpolar hydrocarbon chains, so that the water only sees the ends of the hydrocarbon chains. To show the dramatic effect extremely thin layers of grease contamination can have, the deposition of only one monolayer of myristic acid (molecular chain lying flat on the surface) increased the contact angle by 36 degrees and decreased the lapshear bond strength by 324 psi (2234 kPa).

3.2 Surface Potential Difference (SPD):

3.2.1 Theoretcial Principles:

3.2.1.1 The relationship between SPD and a continuous dipole sheet on the surface has been developed from elementary electrostatics and is known as the Helmholtz equation:

$$SPD = \pm 4\pi\mu\Gamma \qquad (7)$$

In Eq(7), Γ is the number of dipoles per cm^2 and μ is the dipole moment of each dipole. The dipole moment is composed of permanent dipoles and induced dipoles associated with a molecule. For example the myristic acid referred to previously is composed of a carboxyl head group and a hydrocarbon tail of 13 carbon-hydrogen groups as follows:

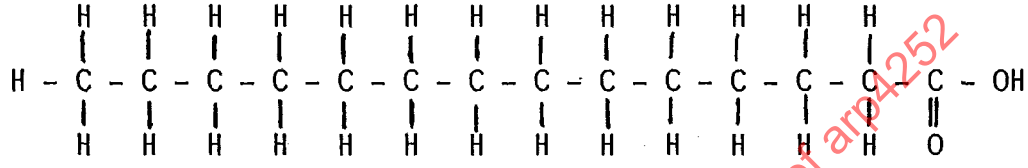

The carboxyl acid group, COOH, at the end has a permanent separation of charge (dipole moment) and each CH group has an induced dipole. The dipole moment μ for the molecule is the sum of these dipoles and depends upon the molecular orientation of the molecule.

3.2.2 Examples of SPD:

3.2.2.1 The SPD vs dip number in Figure 7 illustrates the effect of Γ and μ. The aluminum mirror had approximately 60 Å of oxide prior to dipping through the myristic acid layer. This oxide had a positive SPD value of about 0.7(V). The decrease in SPD between 0 and 1 dip is due to growth of the oxide or hydroxide layer from 60 Å to about 90 Å as the sample was dipped into water without the myristic acid on the water. The first dip increased SPD about 0.1(V) due to the deposition of about 11 Å of myristic acid. The molecules are partly lying flat and partly standing on the head group. Three dips deposits all the myristic acid that can be deposited, with associated increase in SPD. Continued dipping causes rearrangement of the dipoles as observed by the following SPD decrease.

3.2.2.2 Figure 8 shows an example of the use of SPD for relatively thick films. Figure 8 gives SPD vs film thickness (and anodic voltage) for freshly anodized 7075-T6 aluminum alloy and 2024-T3 aluminum alloy and anodized 7075-T6 aluminum alloy after aging. The freshly anodized metal had a water contact angle of zero. The aged sample had a water contact angle of 50 degrees, indicating some contamination with aging. The presence of contamination, although increasing the water contact angle, has not changed the slope of the SPD vs thickness curve. On the other hand, the slope of the SPD vs thickness curve for 2024-T3 is quite different than for 7075-T6, indicating a different effect of the hydroxide film on the dielectric properties of the outer layers.

3.3 Ellipsometry:

3.3.1 Theoretical Principles:

3.3.1.1 Figure 5a shows the components and arrangement of a standard nulling ellipsometer. Starting from the left of Figure 5a, the beam from a light source is passed through a filter to provide a monochromatic beam which then passes through a polarizer to obtain plane polarized light. If this beam is reflected from a specular reflecting surface, the reflected beam is elliptically polarized. The state of ellipticity of the reflected beam contains information with respect to the optical parameters of the substrate and any films that may be on the surface. The interpretation of the state of ellipticity of the reflected light is used to determine the optical properties of the surface, and thus the name of the instrument has become Ellipsometer.

3.3.1.2 In order to simplify the interpretation of the polarization state, a compensator (quarter wave plate) provides elliptically polarized light. The ellipticity of this incident beam can be controlled by the orientation of the polarizer. On the right side of Figure 5d, there is an analyzer (just another polarizer) and photodetector. To make measurements, the compensator is set to ±45 degrees with respect to the plane of incidence (POI) and the polarizer is rotated until the reflected beam is plane polarized. The analyzer can only extinguish the light if polarizer and compensator produce the reflected plane polarization. The readings of the polarizer and analyzer azimuths yield two parameters, Δ and ψ that are directly related to the optical properties of the surface.

3.3.1.3 The elliptically polarized light can be resolved into two orthogonal plane polarized beams, one parallel to the POI and the other perpendicular to the POI. If these two orthogonal beams are in phase with each other, the beam is plane polarized; if not, the beam is elliptically polarized. Δ is the phase shift of the parallel beam with respect to the perpendicular beam, upon reflection of the light. The tangent of ψ is the ratio of amplitudes of these two orthogonal beams (i.e. the ratio of the major and minor axes of the ellipse).

3.3.1.4 The ellipsometric equation that relates Δ and ψ to the optical properties is:

$$RHO=Tan\ \psi\ exp(i\Delta) \quad (8)$$

where RHO is the complex reflection coefficient and $i = \sqrt{-1}$, the symbol for imaginary numbers.

The complex reflection coefficient is:

$$RHO=f(N_s,\chi_s,N_f,\chi_f,d,\lambda,\Theta) \quad (9)$$

where N_s is the substrate refractive index, χ_s is the substrate absorption index, N_f is the film refractive index, χ_f is the film absorption index, d is the film thickness, λ is the light wave length and Θ is the angle of incidence of the light beam. If the substrate has no film, the ellipsometer can be used to measure N_s and χ_s. If N_s and χ_s are known, and the film is transparent, i.e., $\chi_f = 0$, then the ellipsometer can be used to measure the film thickness d and the refractive index N_f.

3.3.1.5 If the film is absorbing and χ_f is not known, then there are three unknowns and only two measured parameters. In order to compute values for the three unknowns, it is necessary to provide at least three independent measured parameters by using two wave lengths or by making measurements with the sample in a medium with refractive index different than air (e.g., water or a solvent), or at least two angles of incidence to obtain a second independent set of Δ and ψ. The theory of ellipsometry and measurement techniques can be found in Ref. 6.

3.3.2 Examples of Ellipsometry:

3.3.2.1 The ability of ellipsometry to nondestructively measure partial monolayers of contamination to films as thick as 6000 nm makes this instrument an extremely useful technique for surface quality assurance. Figure 7 shows a plot of Δ and ψ for extremely thin layers of myristic acid on an aluminum mirror. Dipping the mirror in clean water prior to placing a monolayer of myristic acid on the water surface decreased Δ by about 3 degrees which corresponds to an increase in oxide thickness of about 1.5 to 2.0 nm (i.e., 3 to 4 atomic layers). Note that during these dips, the water contact angle remained very low and the SPD decreased, consistent with the growth of dipoles with negative end pointing away from the surface O = or CH-). The ellipsometer reveals (Figure 7) that after the third dip through myristic acid the film was about 3.5 - 5.0 nm (about the thickness of a bilayer).

3.3.2.2 Measurements of oxide thickness on silicon wafers between approximately 500 Å and 11,000 Å are reported in Table 2 for the fourth type TBE (tri-beam) ellipsometer. The error column reports the percent deviation of the measurements with one TBE (tri-beam) ellipsometer from a standard manual nulling ellipsometer. The values of Δ and ψ at the two wavelengths 750 nm and 810 nm are also given in Table 2. Since the TBE (tri-beam) ellipsometer used two wave lengths, the correct film thickness was computed in each case, even though the film thickness passed through 0, 1st and 2nd order.

3.3.2.3 Table 3 reports surface quality assurance results for phosphoric acid anodized (PAA) 7075-T6 aluminum alloy that had been prepared for adhesive bonding. The results in Table 3 were measured with a TRI-BEAM ellipsometer. The acceptance window of Δ = 152 to 182 degrees was first measured with samples that were known to be properly anodized. The first five samples in Table 3 were properly anodized, whereas numbers 6 and 7 were contaminated with finger prints. Sample 8 was degreased but not anodized. In each case the contaminated or improperly prepared samples were rejected.

3.4 Photo Electron Emission (OSEE):

3.4.1 Theoretical Principles:

3.4.1.1 Optically Stimulated Electron Emission (OSEE) in vacuum is a well established technique, but OSEE in ambient atmosphere has only recently been used for surface quality assurance. To illustrate the principles of OSEE in air, Figure 6 is presented as a simplified schematic representation of the photoelectron emission system. The UV light passes through the collector grid to the sample. The bias between the sample and the collector drives the emitted electrons to the collector by a diffusion process.

3.4.1.2 By using the appropriate light wavelength, emission from the metal substrate can be separated from emission from the oxide layers. For example, let x be the distance in the oxide perpendicular to the plane of the substrate, x=o at the gas-oxide interface and $x=x_o$ at the oxide-metal interface. It is assumed that attenuation of the light in the oxide, compared to total light flux, is small for the oxide thicknesses under consideration. Let P(x) be the escape probability of electrons from position x in the oxide, per unit length, averaged with respect to energy; N_p the number of incident photons per second; P_o the probability of photon absorption at x in the oxide; P_m the probability of photon absorption in the metal; Y_o the number of emitted electrons per absorbed photon in the oxide, Y_m the number of emitted electrons per absorbed photon in the metal; and Θ the fraction of emitted electrons that are collected (includes geometric and field effects due to imposed potential between sample and collector). The probability that an electron will escape from position x in the oxide can be expressed in exponential form as:

3.4.1.2 (Continued):

$$P(x) = C_o \exp(-\bar{x}'/L) \tag{10}$$

where Co is a factor that depends on the work function of the oxide and L is the attenuation length, characteristic of the average energy of the excited electrons. $\bar{x}$ is the distance along the direction with respect to the surface normal (i.e., $\bar{x} = x/\cos\Theta$). The average distance $\bar{x}'$ is:

$$\bar{x}' = \left[\int_{-\Theta_0}^{\Theta_0} (x/\cos\Theta)\, d\Theta\right]/2\Theta_o, \tag{11}$$

where electrons are collected within solid angle Θ about Θ_o
Equation (10) becomes:

$$P(x) = C_o \exp(-x/L'), \tag{12}$$

where

$$L' = L\ell n \frac{\tan(1/4\pi + 1/2\,\Theta_0)}{\tan(1/4\pi - 1/2\,\Theta_0)} \tag{13}$$

The photocurrent Ip can be expressed as:

$$I_P = \left[\int_0^{x_o/L'} GN_P P_o Y_o P(s) d(x/L') + GN_P P_m Y_m P(x_o)\right] \tag{14}$$

where the first term on the right-hand side of Eq. (14) is for electron emission from the oxide, and the second term is for the emission from the metal. Integration of Eq. (14) after substituting for P(x) from Eq. (12) yields:

$$I_p = GN_P C_o P_o Y_o [1 - \exp(-x_o/L')] + GN_P P_m Y_m \exp(-x_o/L') \tag{15}$$

Collecting constants, Eq. (15) becomes:

$$I_P = I_{PO}^{O} [1 - \exp(-x_o/L')] + I_{pm}^{O} \exp(-x_o/L') \tag{16}$$

where

$$I_{P_o}^{O} \equiv GN_P C_o P_o Y_o \qquad I_{pm}^{O} \equiv GN_P C_o P_o Y_m \tag{17}$$

$$\text{At } x_o \ll L', \; I_p = I_{pm}^{O}, \text{ and at } x_o \gg L', \; I_p = I_{P_o}^{O} \tag{18}$$

In the case of a film that does not emit, on a metal that does emit, Eq. (16) reduces to:

$$I_p = I^0_{pm} \exp(-x_0/L') \quad (19)$$

For the case of an emitting film on a nonemitting metal, Eq. (16) reduces to:

$$I_p = I^0_{po} [1 - \exp(-x_0/L')] \quad (20)$$

Equations (10) - (20) are valid for OSEE in vacumm.

3.4.1.3 There are two aspects to OSEE in air; one has to do with the charge carriers (gap resistance) and the other has to do with the driving potential or the field between the electrodes. The current must consist of electrons or ions. In the absence of sparks, arcs, glows, ultra high frequency microwaves and chemical action in flames, ions are created in gases by:

1) Photo ejection of electrons from gas molecules or atoms by x-rays or short wavelength ultraviolet light, or by high energy particles such as alpha particles and gamma rays.

2) Ionization due to electrons emitted by photo-or thermionic excitation from solid surfaces.

3.4.1.4 If process 1 is significant, the current is very sensitive to the cathodic material. Since this is not the case, process 2 is the primary process. According to the theory of electrical conduction in gases (Ref. 7, 8), the first Townsend coefficient (number of electron-ion pairs per electron per cm) is zero up to approximately 15,000 (V/cm) for air. Therefore, with 45(V/cm), ionization of the air by photoelectrons can be neglected. The conduction process must be primarily one of free electrons plus contributions of negative O_2^- due to electron attachment and a small contribution from ions due to photoionization.

3.4.1.5 The maximum photoelectron current emitted in vacuum is I_o. In gas some of these electrons are reflected by gas molecules back to the emitting surface. The net electron current across the gap can be expressed (Ref.7):

$$I/I_o = (X/P)K'_e/[1 + (X/P)K'_e] \quad (21)$$

where X is the electric field (volts/cm), P is the gas pressure (torr),

$$K'_e = 3040\, K_e \sqrt{\bar{V}_o} \quad (22)$$

$\bar{V}_o$ is the average emission velocity of the photoelectrons and K_e is the electron mobility. Equation (21) was developed for a uniform field across the gap and shows that in this case the current I can never be larger than the vacuum photo current. For the conditions $(X/P)K'_e \gg 1$,

$$I = I_o K'_e X/P, \quad (23)$$

3.4.1.5 (Continued):

i.e., Ohm's law is approximated and the current is predicted to be inversely proprotional to P as observed. The kinetic energy of photoelectrons can be expressed:

$$1/2\ m\ \bar{v}_o^2 = 0.6\ (h\nu - \phi e) \qquad (24)$$

where ν is the light frequency, h is Planks constant, ϕ is the work function of the cathode, e is the charge of an electron and m is the mass of an electron. The constant, 0.6, accounts for the fact that all electrons will not have the maximum energy. The average velocity is (From Eq. (24):

$$\bar{v}_o = \sqrt{1.2\ (h\nu - \phi e)/m} \qquad (25)$$

From Eqs. (22), (23), (24), (25):

$$I/I_o = [3040\ K_e(E + \phi')/Pd]/\sqrt{1.2(h\nu - e\phi)/m} \qquad (26)$$

where $x = (E + \phi')/d$, E is the applied voltage and d is the distance between electrodes. The contact potential difference, ϕ', is $\phi - \phi_r$, where ϕ_r is the work function of the reference electrode, and is generally less than 1 V, and therefore small with respect to E(~50 V). Although argon and nitrogen do not capture electrons to any extent, oxygen has a large capture cross-section. Therefore in air or oxygen most of the current is carried by O_2^-.

3.4.2 Examples of OSEE:

3.4.2.1 For aluminum, emission occurs from the metal because the photoelectric threshold is 4.2 eV and the light used was about 5 eV. Photoemission does not occur from the oxide because the photoelectric threshold (the work function) is about 8 eV. Therefore, for Al_2O_3/Al, Po = 0 and Eq. (26) reduces to:

$$I_p = I'_{pm} \exp(-x/L') \qquad (27)$$

where

$$I'_{pm} = I^o_{pm}[(x/P)K'_e/(1 + (x/P)K'_e)]$$

The solid circles in Figure 9 represent the anodized aluminum that had been vapor deposited on glass, the solid triangle represents the anodized 1100 aluminum plate, and the open triangle represents the electropolished Al-1100 plate. All the data in Figure 9 fall close to the straight line drawn through the data points except for the electropolished samples. This indicates that the values of I'_{pm} or L' are different for the electropolish film than for the others and this is probably due to structural differences in this film. From Figure 9, except for electropolish film, $I_{pm} = 1.1 \times 10^{-8}$ amps

3.4.2.1 (Continued):

and $L' = 28^{\circ}A$. The fact that I_{pm} is a constant indicates that ϕ is constant. Experimental values of ϕ for anodized aluminum are approximately constant, independent of oxide thickness.

3.4.2.2 The average electron energy associated with L' is not known; however, for a given photon energy the maximum initial energy Em would be[9], $h\nu = (\phi b + Eo)$ where Eo is the electron affinity of the oxide and ϕ_b is the energy barrier at the Al_2O_3-Al interface. Pong [10] estimates $\phi_b = 1.4 \pm 0.7$ ev and Eo = 1 ev. Therefore, for $h\nu \approx 5$ ev (λ = 2500 Å), the maximum initial energy of electrons emitted into the oxide would be Em $\approx$ 2.6 ev. Kanter and Feibelman[11] measured L' at approximately the same initial energy (ie. Em $\approx$ 3 ev). The value of L' of 28 Å is in close agreement with their value of 25 Å.

3.4.2.3 Attenuation of electrons follows an exponential law (see Eq. 19). To establish a quantitative measure of contamination thickness, an experiment was performed to measure L'. An aluminum foil was bonded to a flat surface and cleaned with trichlorotrifluorethane/methylene chloride (TMC) solvent mixture.. Aluminum foil was used to measure L' because of its high OSEE current and its well known optical properties for ellipsometry. RTV 102 contamination was put on the aluminum foil by placing tissue wipes (saturated with 1% RTV 102/TMC solution) on the foil and allowing the solvent to evaporate. The deposited silicone contamination was then smeared uniformly over the surface with a clean dry tissue. To obtain different contamination thickness, the surface was wiped with a dry tissue a number of times. A plot of OSEE vs contamination thickness (from ellipsometry) is given in Figure 10. The theorectical solid curve in Figure 10 was calculated with Eq. 19, where,

$$I'_{pm} = 9 \text{ nA}$$

and

$$L' = 63 \text{ Å}$$

Figure 10 indicates that the theoretical analysis is verified. It follows that, in principle, OSEE is limited to depths of a few hundred Angstroms. However, if thicker films influence the nature of the outer layers, as for SPD (Figure 8), OSEE may show a correlation with the thickness of much thicker films.

3.4.2.4 It is concluded that the measurement of photoemitted electrons from a metal-film system is simple to perform and that these measurements can be very useful for estimating the thickness of very thin films (0-200 Å) if calibration curves, such as Figure 9, have been made.

3.4.2.5 It was discovered that epoxy paints, used on the external tank of the space shuttle, are photoemitting. This discovery led to a nondestructive inspection (NDI) tool for detection of contaminated paint. This was needed because the polyurethane foam insulation was debonding from the paint due to silicone-type contamination.

3.4.2.6 For utilization of the OSEE inspection tool for quantitative quality assurance, adhesion studies were performed to identify the levels of contamination that significantly degrade the bond. The intensity of the OSEE inspection signal, revealed by the contamination map, can then be determined and used to discriminate between areas that should be cleaned and those that do not need to be cleaned.

3.4.2.7 Once the detection technique has been established and the accept/reject signal level determined, it is only a matter of automatically scanning the tanks to produce a map of the surface that reveals those areas that must be cleaned. Remapping after cleaning will reveal if the cleaning has been adequate.

3.4.2.8 An epoxy painted panel was contaminated with silicon RTV 102 as follows: the silicone RTV 102 was dissolved in tetrahydrofurane (THF) and then diluted to make four contamination levels. Pure THF was used for zero contamination, 1 part contaminated solution was added to 3 parts THF to provide 0.25 level, 2 parts were added to THF to provide 0.5 level and undiluted solution was used for level 1. Four tissue papers were each saturated with one of the contamination level solutions and wiped onto the four regions of the painted panel. Figure 10a shows the OSEE as a function of the contamination level. OSEE drops dramatically, and levels off at a low value between contamination level 0.5 to 1.0. The curve in Figure 10b shows the effect of the contamination on the peel force for stripping adhesive tape at a speed of 4 inches/minute (1.7 mm/s) at 180 degrees peel. The peel force follows a curve similar to the OSEE curve, revealing a direct correlation between the OSEE inspection and the resultant adhesion properties of the surface.

3.4.2.9 Painted panels, 1 foot x 1 foot (305 x 305 mm), were divided into 12 regions, as in Figure 12. The lower regions were left uncontaminated as a control. The other regions were contaminated with fingerprints, masking tape residue, 3-in-1 oil, lubrication grease, cotton glove smudge, Kraft paper, smudge, RTV 102, RTV 655, and automobile engine exhaust. The fingerprint area was contaminated by rubbing the fingers over the forehead and then on the panel. The tape area was contaminated by pressing masking tape to the panel and then removing it. RTV 655 was a mix of part A and B dissolved in TMC to make 1% solution, as for the other contaminants. The region identified as car exhaust was held for 30 seconds, 1 foot (305 mm),from the exhaust pipe.

3.4.2.10 An OSEE map of the panel represented in Figure 12 was made and a reduced-thickness (d/L´) map is given in Figure 13. The maximum reduced thickness (i.e., d/L´) is 1.66, so that the maximum contamination thickness is 1.66 x 63 = 105 Å. Figure 13 reveals very little contamination in the control area, the masking tape residue area, the cotton glove and Kraft paper smudge areas and the car exhaust area. The fingerprint, 3-in-1 oil, lube grease, and silicone contaminated regions are strongly revealed.

3.4.2.11 After mapping the panel, half of each area 0.5-inch (12.7 mm) wide, was bonded with masking tape and the other half, 0.5-inch (12.7 mm) wide was bonded with PR-365 polyurethane one-part adhesive. A fiberglass cloth scrim was embedded in the PR-365 for backing strength. The PR-365 was approximately 1/16 inch (1.6 mm) thick. The tape and PR-365 strips were cut with a thin-bladed knife and pulled in 180 degrees peel at 4 inches/minute (1.7 mm/s). The peel forces for the masking tape are indicated in Figure 13. The control area, the masking tape residue, 3-in-1 oil, Kraft paper and car exhaust contaminated areas failed between 490 and 551 g/cm. The cotton glove smudge area failed at 433 g/cm, the lube grease contaminated area at 393 g/cm, the fingerprint contaminated area at 299 g/cm and the silicone contaminated area at less than 10 g/cm. The PR 365 formed strong bonds (> 4.3 to 5.1 kg/cm) in all except the silicone contaminated areas, where the peel strength was approximately 0.3 kg/cm. The bond peel strength in areas other than silicone contamination was actually greater than 4.3 to 5.1 kg/cm because failure was at the glass scrim rather than the paint interface. The silicone contaminated regions failed at the paint-adhesive interface.

3.4.2.12 Table 4 gives a few of the applications for which OSEE has been excellent.

REFERENCES

1. T. Smith and G. Lindberg, Surface Technology, 9, 1 (1979).
2. H. Palevsky, R. K. Swank and R. Grenchik, Rev. Sci, Inst. 18, 298 (1947).
3. T. Smith, J. Electroanal. Chem. 150, 277, (1983).
4. T. Smith, Surface Science, 56, 212 (1976).
5. T. Smith, "Mechanisms of Adhesion Failure between Polymers and Metallic Substrates" Technical Report AFML-TR-74-73, June 1974.
6. F.L. McCrackin et al, NBS Journal of Research, 67A No. 4, 363 (1963).
7. L. B. Loeb, "Basic Process of Gaseous Electronics", University of California Press, 666 (1961).
8. O. H. DeBoer, "Electronic Emission and Adsorption Phenomena," Cambridge, 12 (1935).
9. R. J. Powell, U.S. Army Research Office, Durham N.C. Tech. Report No. 5220-1 (SU-SEL-67-032), (1967).
10. W. Pong, J. Appl. Phys. 40, 1733 (1969).
11. H. Kanter and W. A. Feibelman, J. Appl. Phys. 33, 3580 (1962).

Table 1 - Surface Inspection Instruments

	Wettability	SPD Surface Potential Diff.	Ellipsometry	OSEE Photoelectron Emission
Principle	Oleophilic nature	Number & Orientation of Dipoles.	Reflection of Polarized Light.	UV Light emission of electrons in air.
What is measured	Water contact Angle	Voltage between ref. electrode & surface	Film Thickness Film refractive Index.	Photoelectron current Film Thick, Emission Coef. Attenuation Coef.
Approximate Depth of Measurement	0 to one molecular Layer (~1 nm)	0 to one molecular Layer (~1 nm)	0 to 6000 nm	0 to 100 nm
Field Application	Yes	Yes	type 4 only	Yes
Estimated Proficiency Level to operate	Basic	Basic	Average	Basic
Estimated Proficiency Level to Interpret Results	Basic	Average	High	Average
Est. Cost Range in $1000	0 - 6	3	15 - 90	10 - 16

Table 2

TEST # 0 :SIO2/SI 8 SAMPLES FROM SQC

ANGLE OF INCIDENCE = 60 WAVELENGTHS = 7500, 8100 Å
No. OF INTIAL FILMS = 0
WL=750 NS=3.71 KS=0.0016 NF=1.46 KF=0.00
WL=810 NS=3.69 KS=0.0008 NF=1.46 KF=0.00

TABLE OF MEASURED FILM THICKNESS

No.	DEL(750)	DEL(810)	PSI(750)	PSI(810)	FILM THK	% ERROR
1	141	143	24.9	25.3	477	0.7
2	110	118	36.6	34.4	1063	2.9
3	193	211	23.3	25.5	3041	0.1
4	247	221	33.6	57.5	5367	0.3
5	124	122	55.9	31.0	7774	-0.1
6	250	119	54.2	44.4	8225	-0.6
7	161	216	23.3	26.2	9821	-0.1
8	131	129	55.9	28.5	11026	-0.4

Table 3

TEST # 7 :

ANGLE OF INCIDENCE= 60 WAVELENGTHS= 7500, 8100 Å
NO. OF INITIAL FILMS= 0

QUALITY ASSURANCE INSPECTION OF SURFACE
FOR 30 CYCLES
ACCEPTANCE WINDOW= 151 TO 182

MEASUREMENT	DELTA		ACCEPT OR REJECT
1	172	Proper PAA	ACCEPT
2	180	" "	ACCEPT
3	180	" "	ACCEPT
4	158	" "	ACCEPT
5	167	" "	ACCEPT
6	106	Finger Print	REJECT
7	106	" "	REJECT
8	123	Not Anodized	REJECT

Table 4

Applications and Surfaces Successfully Inspected by OSEE

General Applications

1. Bare metal surfaces after various surface treatments in preparation for painting, adhesive bonding, soldering, etc.
2. Painted surfaces where the paint and substrates are good or very slight conductors. For example, metals, semiconductors, most polymers, but not cellulosic or highly insulating materials.
3. Graphite/epoxy composites; it should work as well on any epoxy composites, e.g., with glass, ceramic, or metal fibers.
4. Inspection of semiconductor surfaces for contamination or process errors.

Specific Applications

1. Metal oxide thickness monitors, Al_2O_3 /Al, NiO/Ni, etc.
2. Surface contamination on aluminum with and without epoxy paint.
3. NDI of ball bearings.
4. NDI of metal sheets for cold weld lamination, Al, Ni, Zn, steel, Cu, brass, Ti, Be.
5. NDI of epoxy composites.
6. NDI for soldering semi-conductor chips to lead frames and power transistors to heat sinks.
7. NDI of semiconductor surfaces, Hg-Cd, Hg-Cd-Te.
8. NDI of silicon wafer for contamination, dust and photoresist.
9. Surface properties for ZnS/sapphire.
10. NDI of scratch defects on aluminum sheet.
11. Properties of lithographic plates.

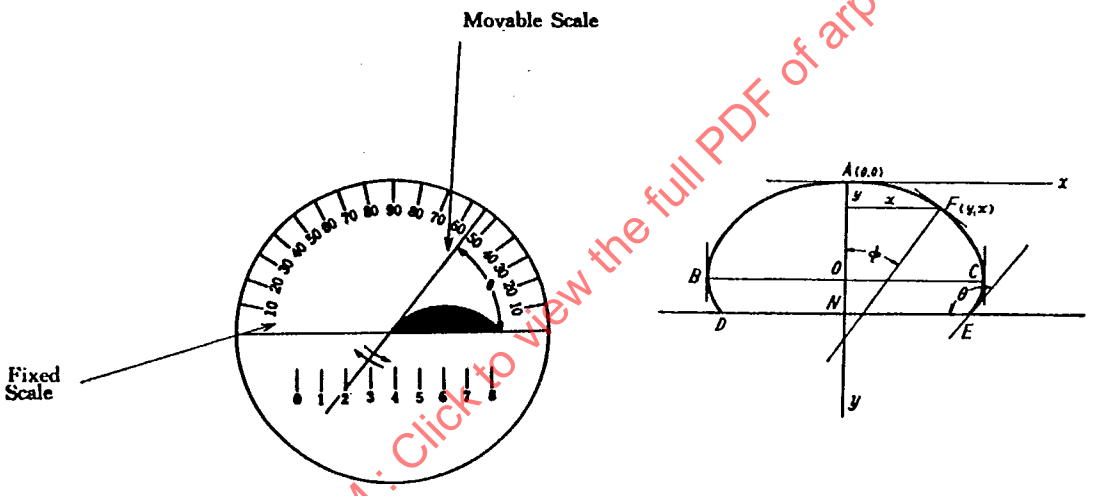

(a) Direct reading Goniometer

(b) Ordinary drop shadow

FIGURE 1 - Goniometer Reading of Contact Angle

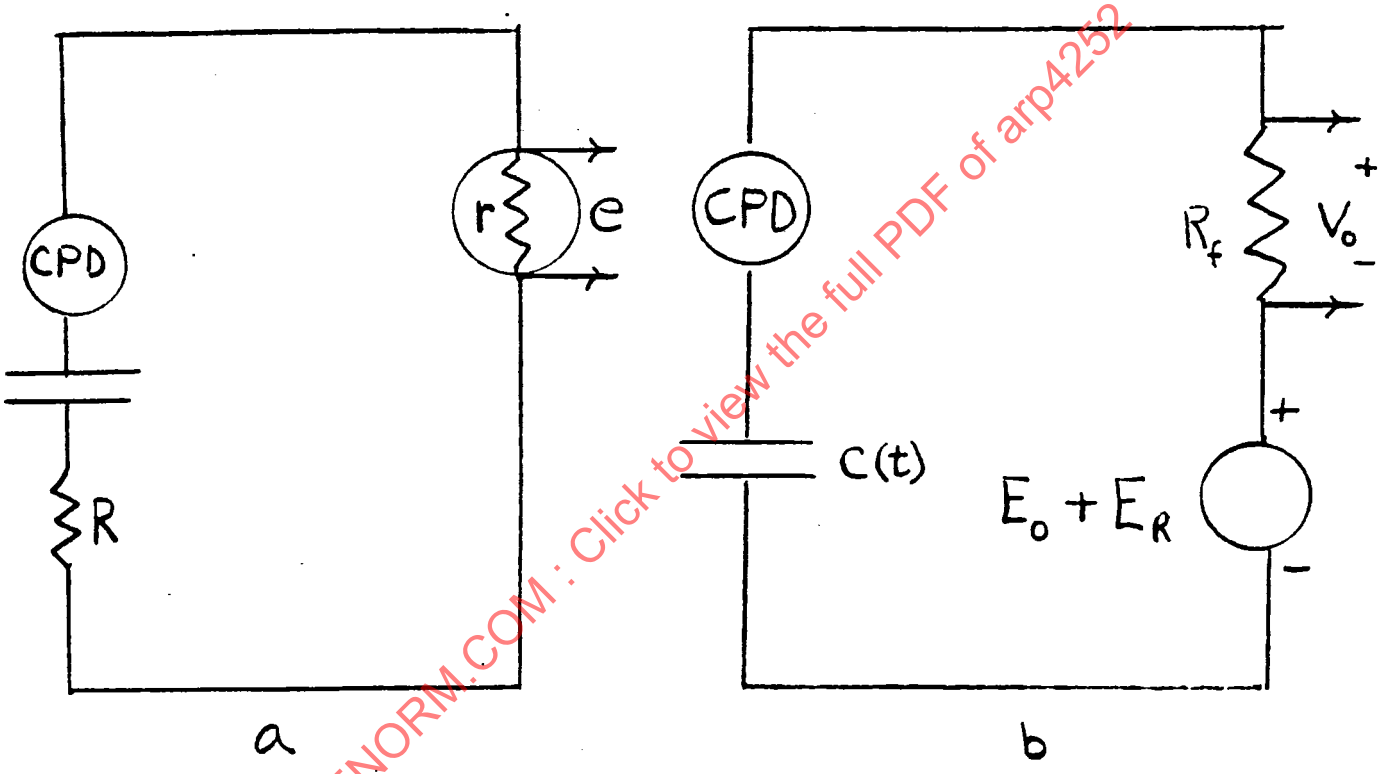

FIGURE 2 - Schematic Electrical Equivalent Circuits

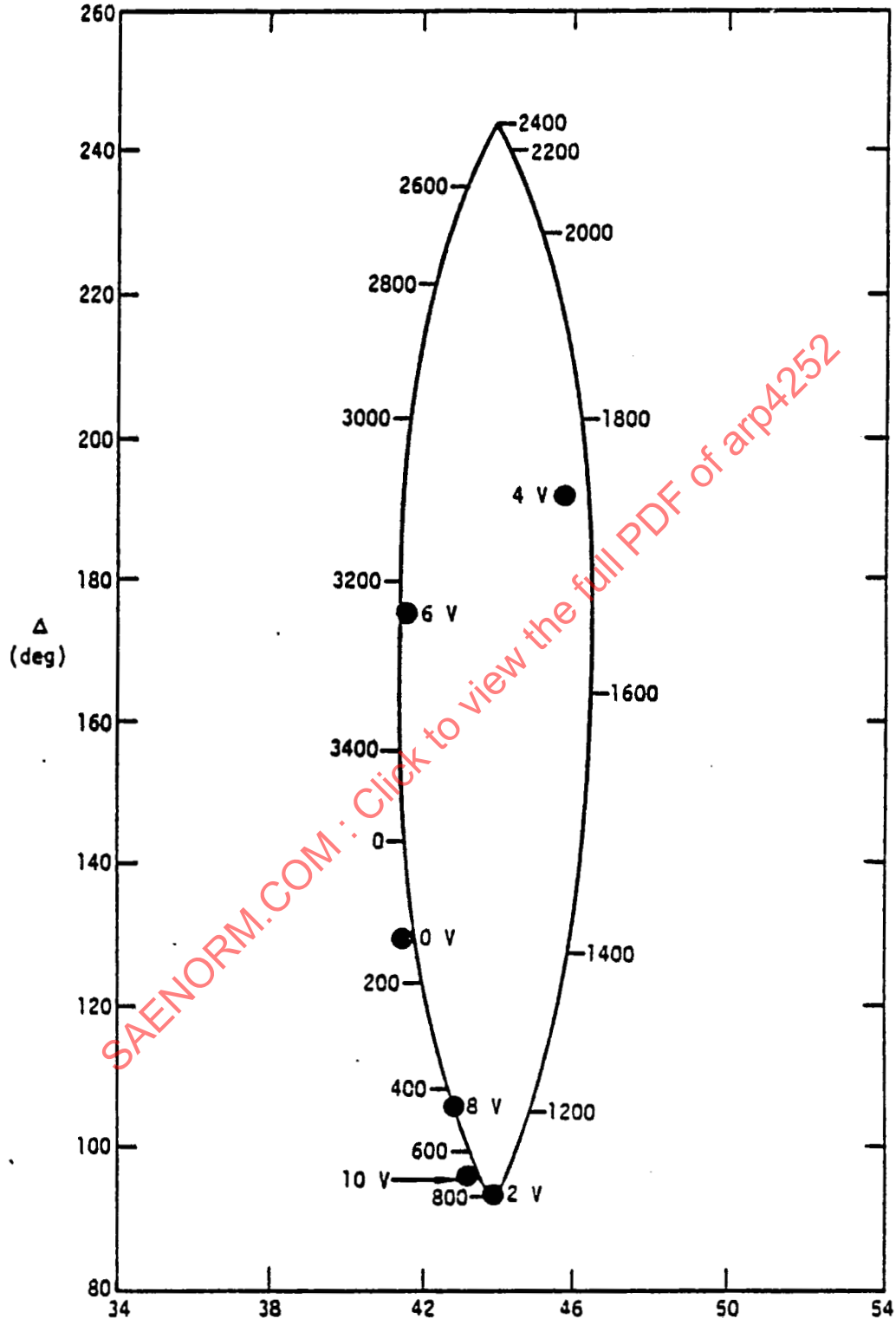

FIGURE 3 - Δ vs. ψ plot for a theoretical film (curve) of refractive index 1.3 and thicknesses indicated. The solid circles are experimental data for phosphoric acid anodized Al 1100 that had been previously electropolished to smooth the surface.

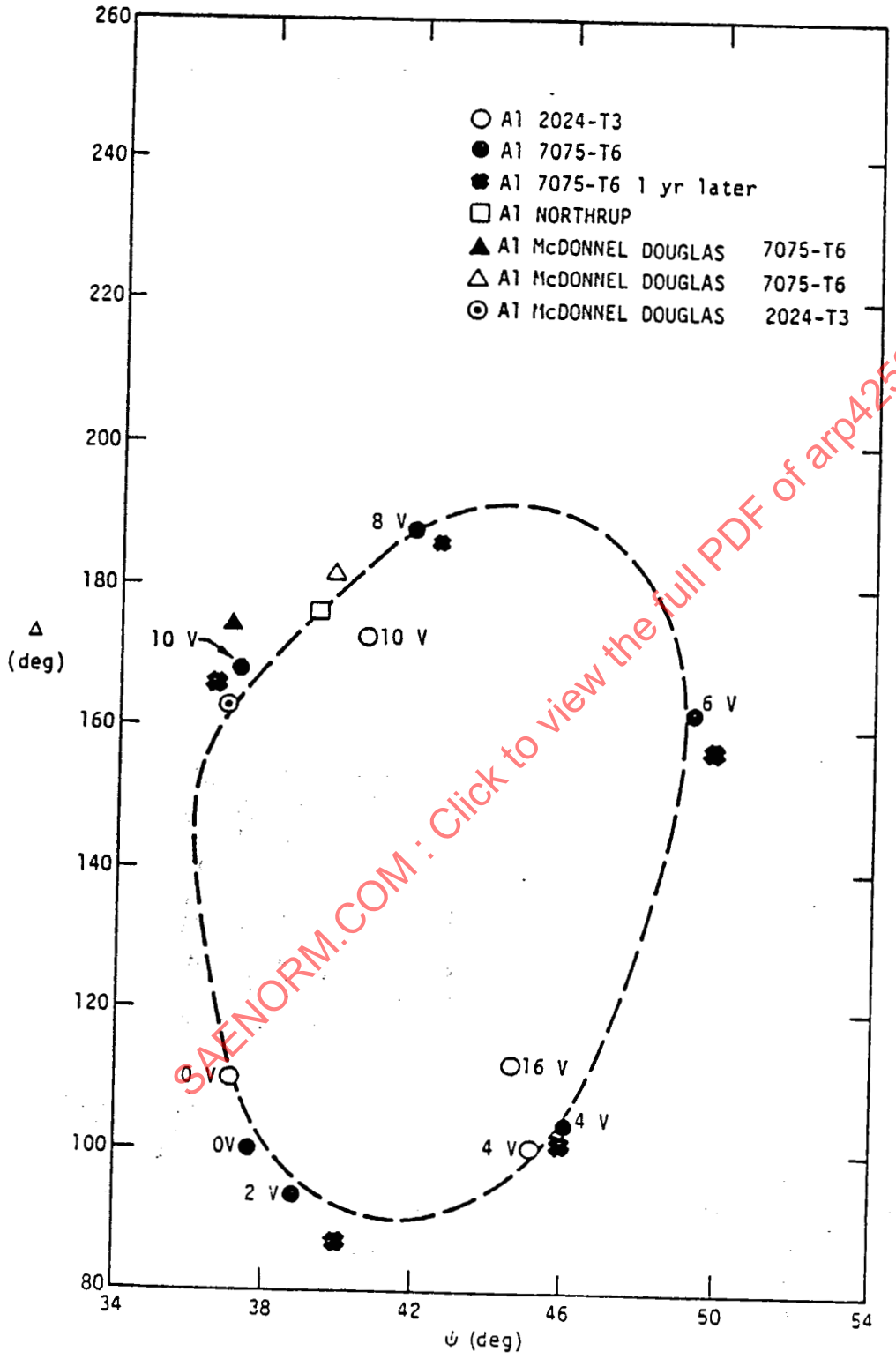

FIGURE 4 - Δ vs. ψ plot for rough 7075-T6 and 2024-T3 aluminum alloy anodized samples (at the indicated voltage for 22 minutes), λ = 6328 Å, ϕ = 70°

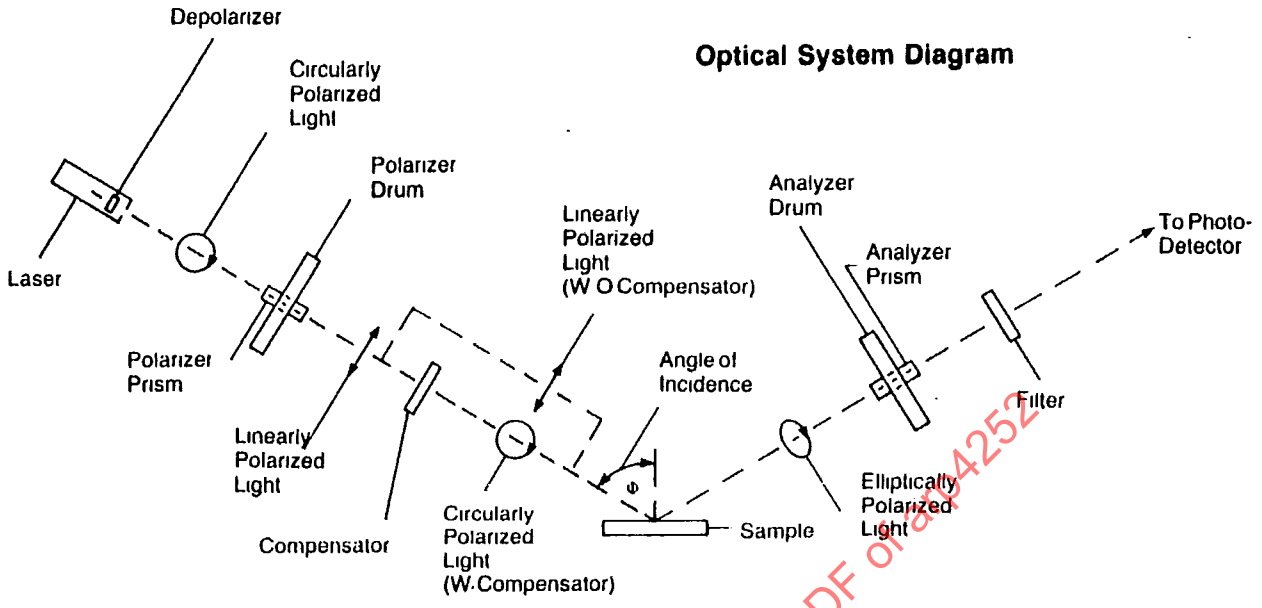

FIGURE 5a - Optical Arrangement of Nulling Ellipsometer

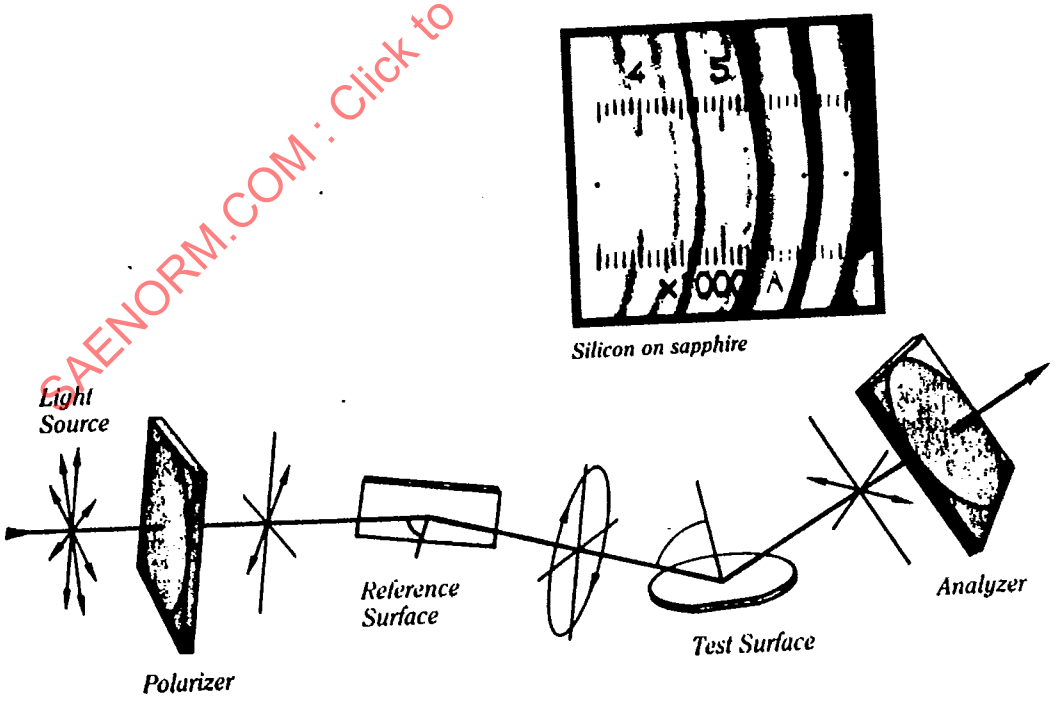

FIGURE 5b - Optical Arrangement of Comparison Ellipsometer